

Supplementary Figures and Tables

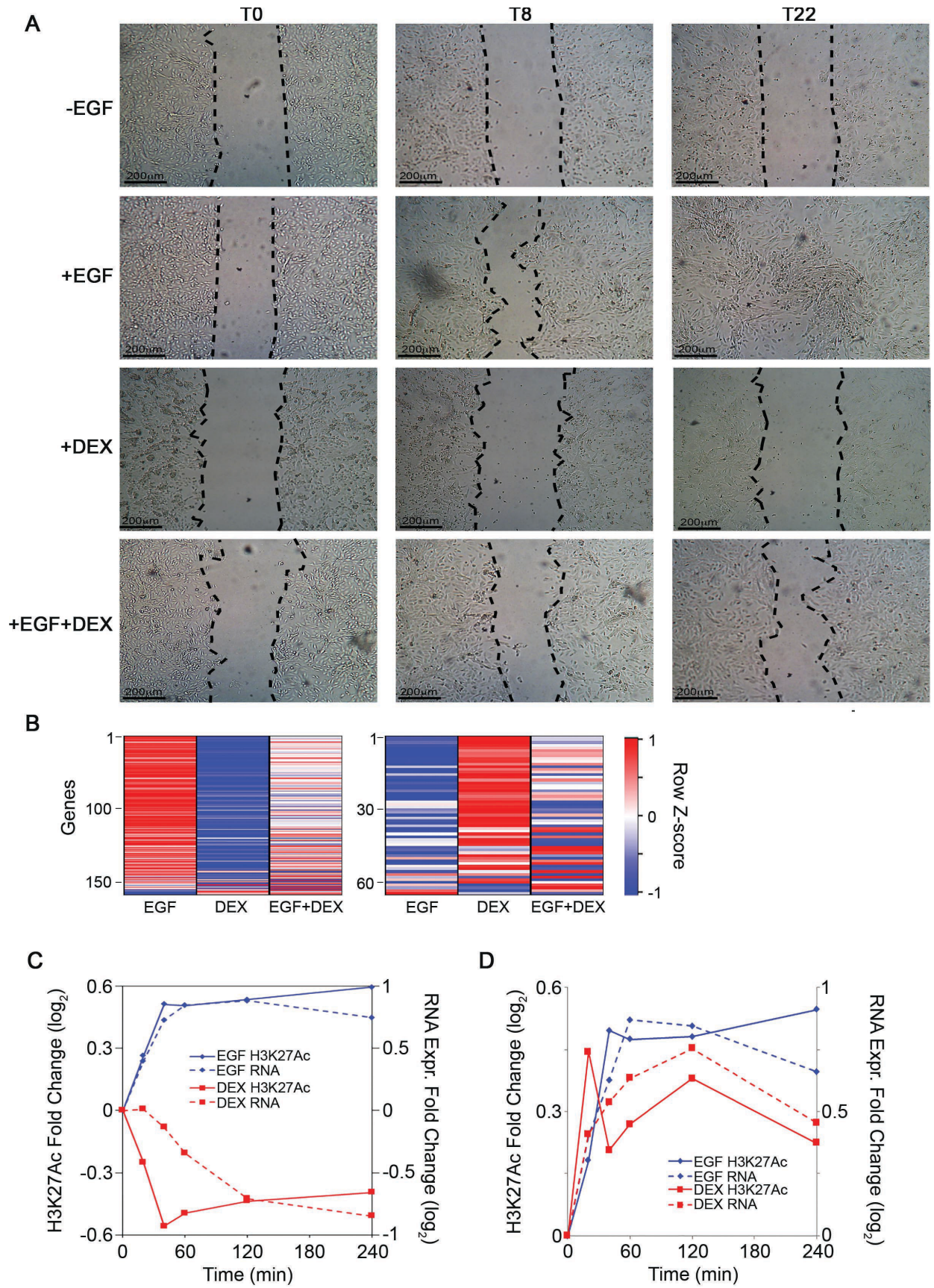


Figure S1: Dexamethasone, a glucocorticoid analog, inhibits EGF-induced migration and extensively modifies transcription and H3K27Ac occupancy in human mammary cells. (A) MCF10A human mammary cells were plated in plastic inserts (8×10^5 cells). Following an overnight incubation, the plastic barriers were removed and cells were treated without or with EGF (10 ng/ml), DEX (100 nM), or a combination of EGF and DEX. Three representative time frames are shown for each treatment (0, 8 and 22 hours). Dashed lines mark migration fronts. Scale bar 0.2 micrometer. (B) A heatmap showing RNA expression alterations occurring in MCF10A cells in response to EGF, DEX, or a combination of both, following 60 min of stimulation. Shown are 165 (left panel) and 66 (right panel) genes, which underwent either up- or down-regulation, respectively, by >0.7 fold change (\log_2 scale) relative to un-stimulated cells. Z-scores of individual genes (rows) are presented, meaning that each gene (row) was forced to have a mean of 0 and standard deviation of 1. Notably, the genes were selected only according to their response to EGF and, therefore, a minority of these genes are also affected in the same way by both EGF and DEX treatment. Hence, the apparent “non-coherent” colors in the heatmap. Additionally, Z-scores were used only for presentation of the heatmaps. (C) MCF10A human mammary epithelial cells were starved overnight for serum factors. Thereafter, they were treated with EGF (10 ng/ml), or with DEX (100 nM), for 20, 40, 60, 120 and 240 minutes. ChIP-Seq tag reads were tallied near promoter regions (defined as ± 3 kb relative to the TSS). Shown is a time series of average alterations in H3K27Ac occupancy and RNA abundance of 45 module B (EGF^{UP}/DEX^{DOWN}) genes. (D) Shown is a time series similar to C, except that 14 module A (EGF^{UP}/DEX^{UP}) genes are presented. Note that alterations in the occupancy of H3K27Ac in response to EGF or DEX are highly concordant with mRNA expression alterations. In addition, the H3K27Ac occupancy alterations tend to be more rapid, such that they precede the corresponding mRNA alterations.

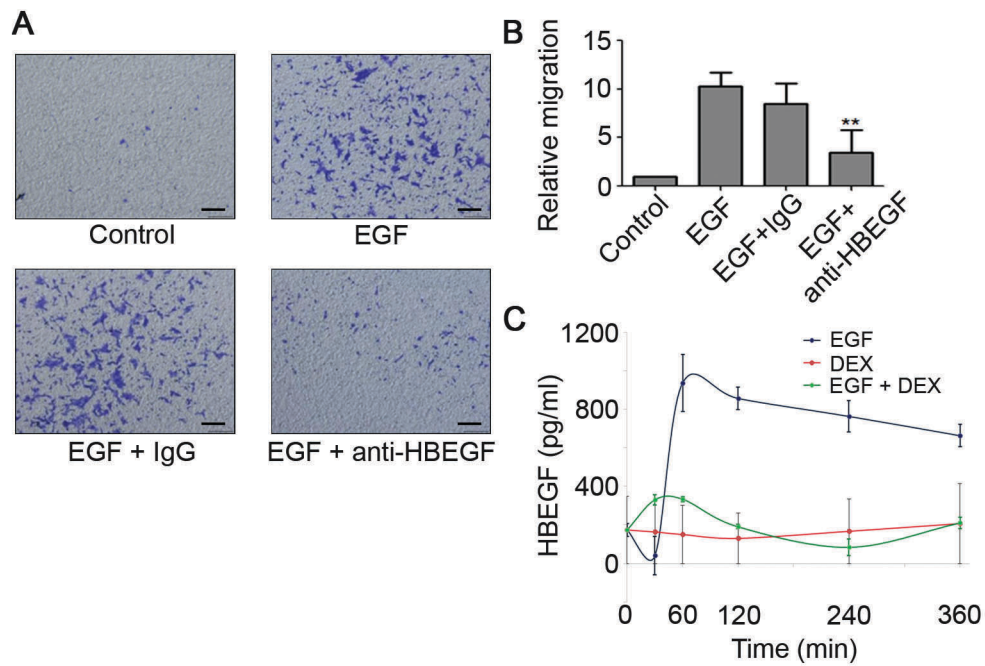


Figure S2: Role for HBEGF in sustaining migration of MCF10A cells. MCF10A cells were starved overnight. (A) Following starvation for serum factors, 40,000 cells were seeded in transwell compartments for migration assays under the indicated treatments. (EGF: 10 ng/ml, antibodies: 20 ug/ml). Immunoglobulin G (IgG) was used as negative control. Shown are representative images of two biological replicates. Scale bar, 200 μ m. (B) Relative quantification of cell migration, where $n=2$, $p<0.01$. (C) MCF10A cells (2×10^6) were seeded in 10-cm plates and 24 hours later they were starved for 12 hours. Thereafter, cells were stimulated with EGF (10 ng/ml), DEX (100 nM), or the combination, for the indicated time periods. Cells were then washed and lysed in RIPA buffer (50mM Tris, pH 7.5, 150mM NaCl, 1% NP40, 0.1% SDS, 1mM EDTA and 0.5% sodium deoxycholate). Protein content was estimated using the BCA kit (from Sigma), followed by HBEGF concentration analysis by an ELISA kit (DuoSet ELISA Kit, from R&D Systems, Minneapolis, MN). Shown are HBEGF levels after normalization to the amount of total proteins.

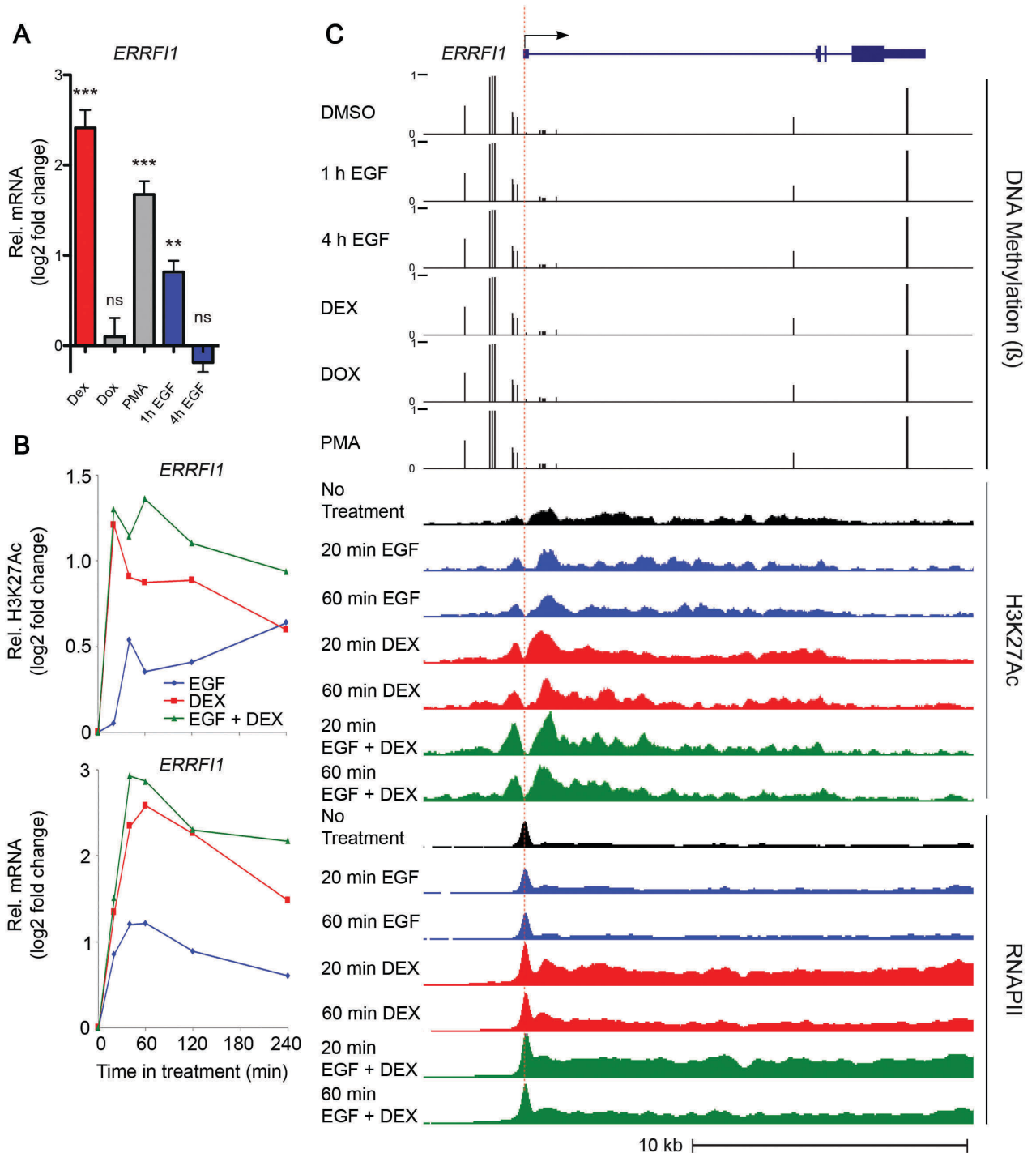


Figure S3: Diverse stimuli alter expression of *ERRF1*, as well as H3K27Ac and RNAPII occupancy levels at the respective TSS, with no detectable effects on DNA methylation levels. (A) MCF10A cells were treated for 60 minutes with dexamethasone (DEX), doxorubicin (Dox), phorbol myristate acetate (PMA), EGF (for 60 minutes or for 4 hours), or with DMSO (solvent control). The abundance of transcripts corresponding to a module A gene, *ERRF1/mig6*, was determined using qPCR and plotted for each condition relative to DMSO control (n=3 for each

treatment). *GAPDH* was used for normalization. * $p < 0.05$, ** $p < 0.01$, *** $p < 0.001$ when compared to DMSO control using one-way Anova with Tukey's post-test. Non-significant (*ns*) differences to control are indicated. **(B)** Time series showing alterations in H3K27Ac occupancy (upper panel) and mRNA levels (lower panel) corresponding to the *ERRF1/mig6* gene. H3K27Ac occupancy and mRNA levels were calculated and presented as in Figures 1B and 1C. **(C)** The genomic structure and TSS (a horizontal arrow and a red vertical dotted line) of *ERRF1/mig6* are shown (top of panel C). DNA methylation in the region of *ERRF1* was determined using Illumina 450K arrays ($n=3$ for each treatment). Methylation values range from 0 (un-methylated) to 1, fully methylated. ChIP-Seq signal tracks are presented as in Figure 1E.

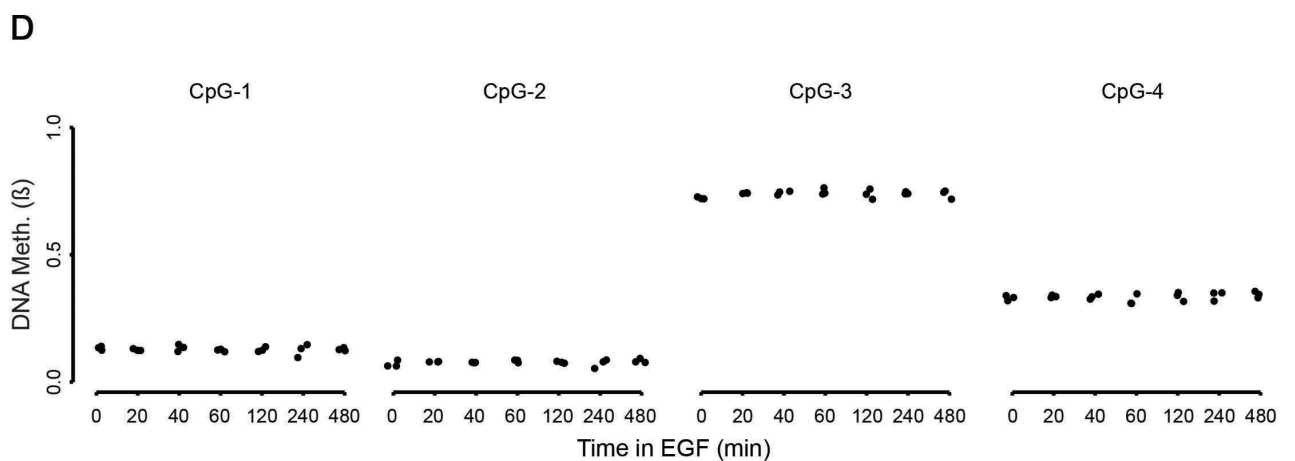
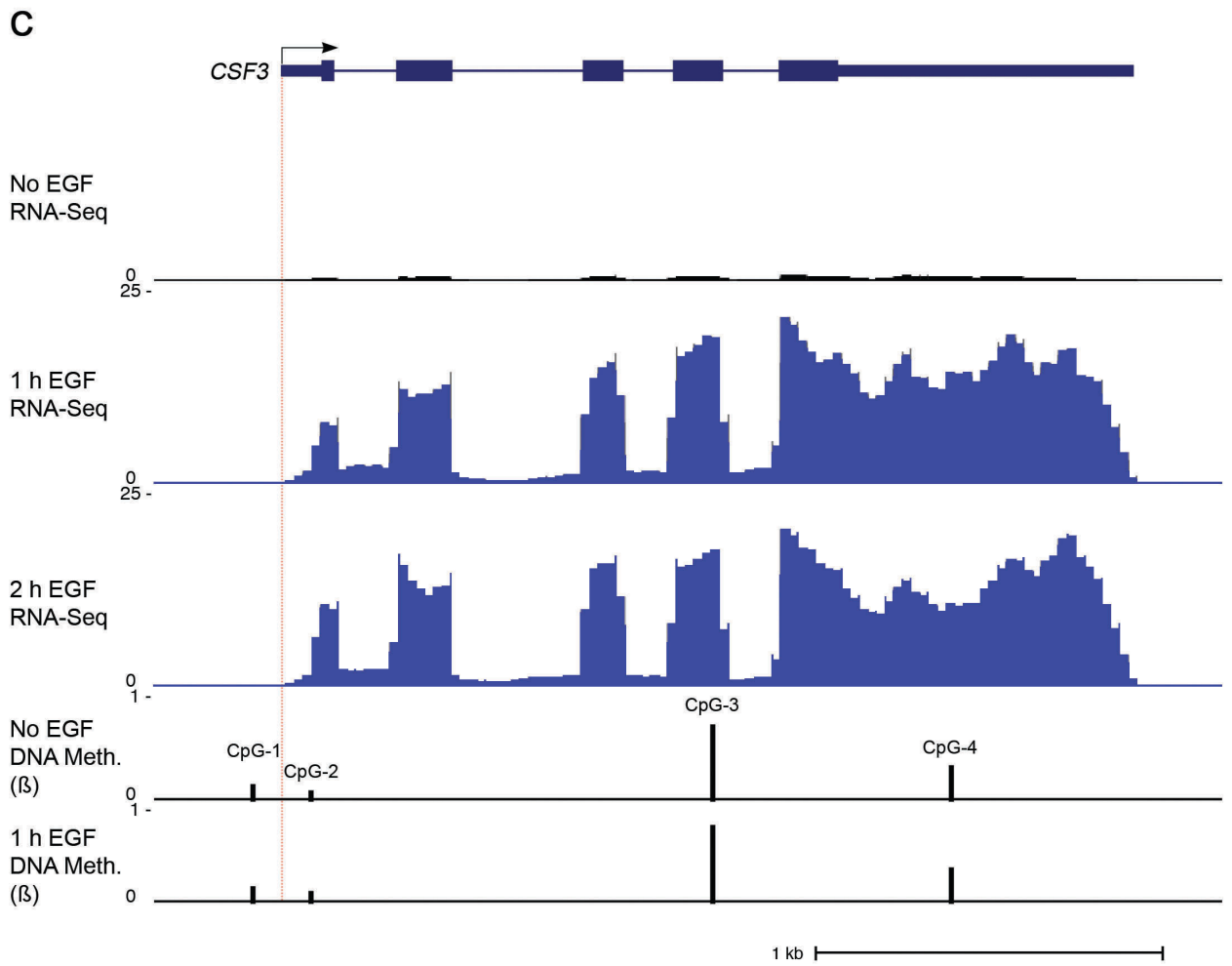
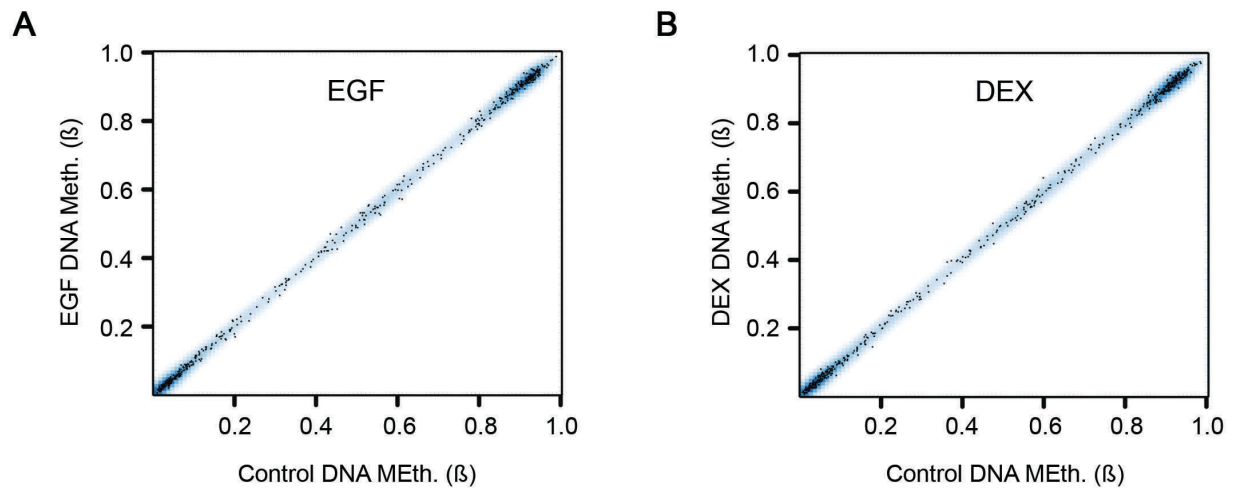


Figure S4: Genome-wide methylation levels are not altered upon short-term treatments with EGF or dexamethasone, even for the strong EGF-mediated induction of *CSF3*. (A) A scatter plot comparing DNA methylation detected in untreated MCF10A cells and in cells treated with EGF for 60 minutes. Dots show methylation levels at 500 randomly selected CpGs, as determined using Illumina 450K arrays (n=3 for each treatment). The blue background depicts the smoothed distribution density based on methylation measurements (n=3 for each treatment) at all 422,743 CpGs included in the Illumina 450K arrays. Zero indicates an un-methylated site, while 1 indicates a CpG site that is fully methylated. (B) A scatter plot similar to A, except that cells were either untreated or treated for 60 minutes with DEX. (C) A scheme presenting genomic regions encoding the colony stimulating factor 3 gene (*CSF3*; top). The horizontal arrow marks the transcription start site (TSS). Exons are shown as bold rectangles and introns as lines. The lower three tracks present transcript levels, based on RNA sequencing, which were determined either prior (*No EGF*) or after stimulation of MCF10A cells for 60 and 120 minutes with EGF. The bottom two tracks depict levels of DNA methylation, as determined using Illumina's 450K BeadChip, before and after 60 minutes of EGF stimulation. Methylation levels range from 0 (un-methylated) to 1 (a fully methylated CpG site). (D) DNA methylation of the 4 CpG dinucleotides from panel A is shown across an extended time course following EGF stimulation (n=3 for each time point).

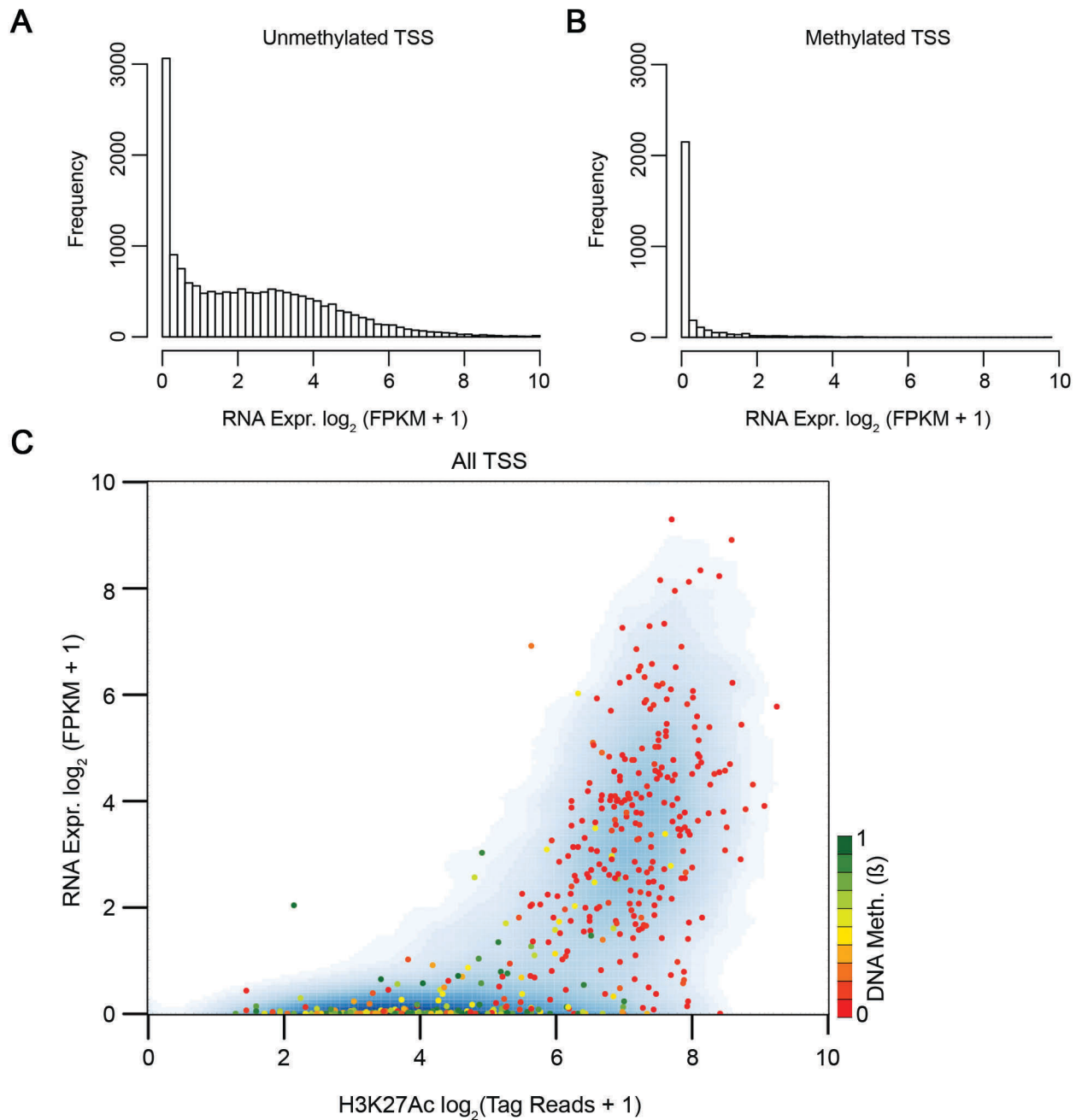


Figure S5: Basal genome-wide DNA methylation levels reciprocally relate to histone 3 acetylation and transcript abundance. (A) A histogram depicting RNA abundance for all of the un-methylated ($\beta \leq 0.15$) TSS of un-stimulated (control) MCF10A cells. TSS were identified by processing RNA-Seq data using TopHat with a reference gene model derived from GENCODE (version 19). Of the 69,211 TSS identified by TopHat, 26,004 have an Illumina 450K CpG measurement within 100 bp of the TSS. (B) A histogram as in A, depicting RNA abundance for all of the methylated ($\beta \geq 0.85$) TSS. Expression and methylation values were derived from MCF10A cells prior to stimulation. (C) A scatter plot of H3K27Ac occupancy versus abundance of the

respective mRNAs of untreated MCF10A cells. Shown in blue is a smoothed distribution density representing 17,180 TSS. Dots are drawn for 500 randomly selected TSS colored according to their DNA methylation levels. ChIP-Seq tag reads were tallied near promoter regions. TSS were identified by processing RNA-Seq data using TopHat with a reference gene model from GENCODE.

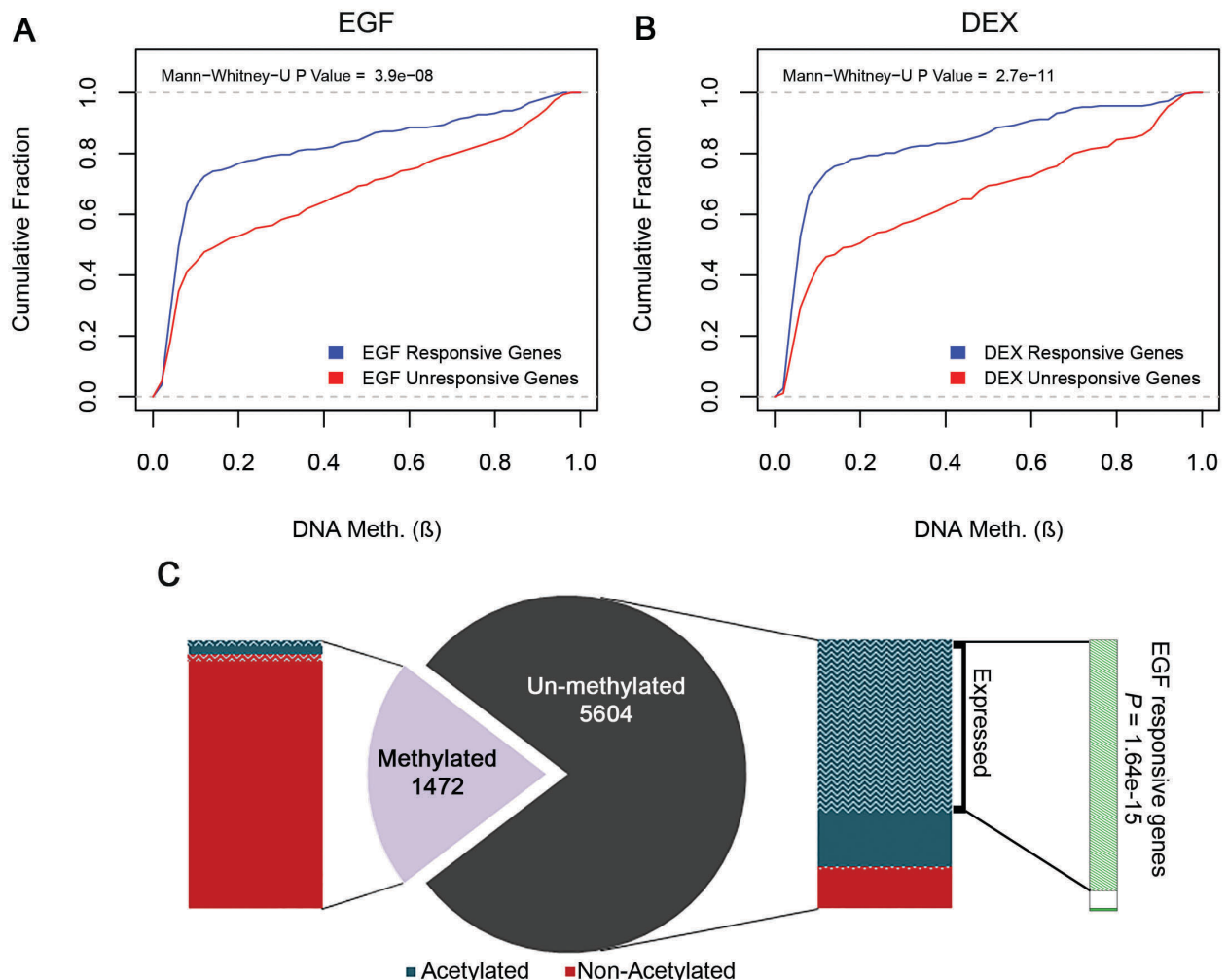


Figure S6: The unmethylated portion of the genome is responsive to EGF, while the methylated part is unresponsive and displays very low basal acetylation of histone 3. (A) Basal DNA methylation levels at promoter regions ($TSS \pm 100$ bp) of EGF-responsive genes ($N = 236$) are compared to methylation levels displayed by genes that are unresponsive to EGF ($N = 443$; see Methods). Note that DNA methylation levels are lower in TSS of EGF-responsive genes relative to the group of genes that are unresponsive to EGF treatment ($p = 3.9 \times 10^{-8}$, Mann-Whitney-U test). Responsive genes are defined as genes whose transcript levels alter (either upward or downward) by more than a factor of 0.6 (in a \log_2 scale) in two consecutive time points. RNA abundance and DNA methylation levels were derived from untreated (control) MCF10A cells. **(B)** Basal DNA

methylation levels at the promoter regions (TSS \pm 100 bp) of DEX-responsive genes (N = 252) are compared to methylation levels displayed by genes that are unresponsive to DEX treatment (N = 264). Note that DNA methylation levels are lower in the TSS of DEX-responsive genes compared to a group of genes that are unresponsive to DEX ($P = 2.7e-11$, Mann-Whitney-U test). Lists of responsive and unresponsive genes were obtained from microarray data previously generated in our lab using MCF10A cells stimulated with EGF (or with DEX) for 20, 40, 60, 120 and 240 minutes. (C) Shown are the distributions of DNA methylation and histone 3 acetylation in TSS regions of 7,076 genes expressed in mammary cells. The expressed fractions are marked by waves. Notably, whereas most (92%) of the 1,472 methylated TSS regions are non-acetylated and un-expressed (FPKM \leq 1), most of the un-methylated TSS regions are acetylated and expressed. The rightmost green bar presents 188 genes that clearly respond to EGF (>2 fold up- or down-regulated after 60 or 120 min treatment). The majority of these genes (hatched segment; 174 genes) belong to the un-methylated, highly acetylated portion of the pie chart and they are included in the “expressed” portion of the right bar. The other 14 genes belong to two less defined subtypes. The p -value was calculated using Pearson's Chi-squared Test.

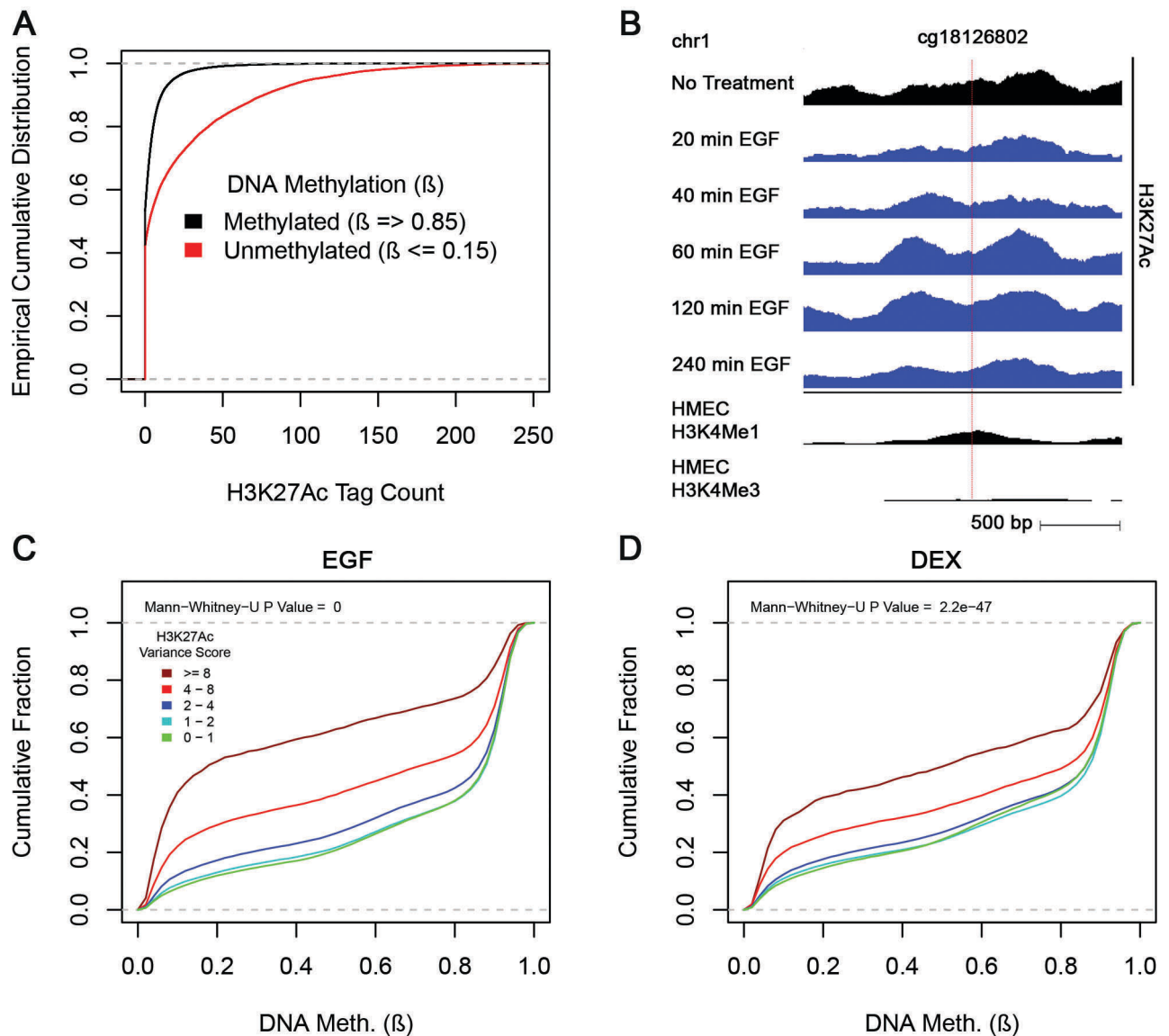


Figure S7: Un-methylated regions distal to TSS of responsive genes are associated with relatively high H3K27Ac occupancy and dynamic alterations in response to EGF. (A) Shown is the Empirical Cumulative Distribution Function (ECDF) of H3K27Ac tag reads in 2000 bp windows, centered on CpG sites, as measured by using the 450K array. H3K27Ac tag reads were calculated using the annotatePeaks.pl from the HOMER suite and input tag reads were subtracted. To focus on CpGs of distal regulatory regions, only those CpGs that have no expressed TSS in MCF10A cells in the range of ± 5 kb from the CpG were included. The numbers of unmethylated and methylated distal regions are 17,863 and 77,556, respectively ($p < 2.23e-308$, Mann-Whitney-U test). (B) Browser views of H3K27Ac ChIP-seq pileup fragments of a 2 kb region of chromosome 1, distal (>5 kb) to TSS and corresponding to the CpG site cg18126802 in the 450k methylation array. Shown are tracks corresponding to five time points following EGF stimulation. The red vertical dotted line indicates the site of the corresponding un-methylated CpG. This CpG site, like

other CpG sites included in our analysis, is located more than 5 kb away from any actively transcribed TSS in MCF10A cells. For reference, published ChIP-seq data of H3K4Me1 and H3K4Me3 for normal human mammary epithelial cells (HMEC), which are similar to MCF10A cells, are shown, suggesting that this site is an enhancer (high H3K4Me1 and low H3K4Me3). (C and D) Shown are basal DNA methylation levels at regions distal to TSS and displaying different degrees of dynamicity (shown by the variance score) in response to either EGF (C) or DEX (D). Note that DNA methylation levels are lower in distal regions that display higher dynamicity (variance score ≥ 8 ; brown line) compared to a group of distal regions unresponsive ($0 \leq$ variance score ≤ 1) to treatment with either EGF or DEX ($p < 1e-100$ and $p = 2.2e-47$, respectively, Mann-Whitney-U test). Lists of DNA regions grouped according to their variance score were obtained as in Figure 6. The cumulative fraction of CpG methylation levels was calculated for 5 categories of variance score (see a color key in the inset of C).

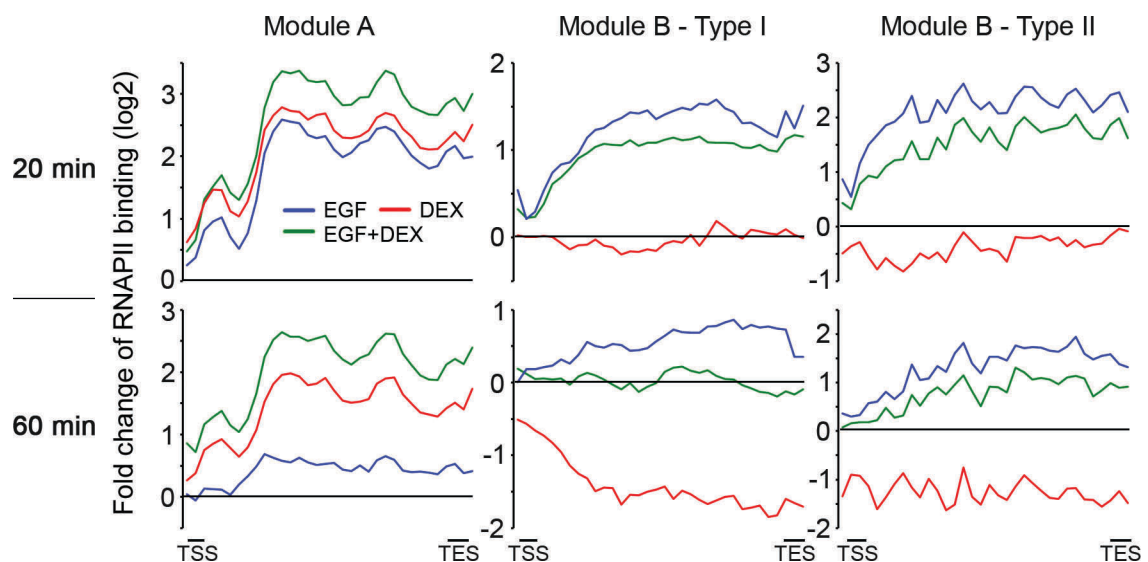


Figure S8: Subgroups of the cooperative and antagonistic modules display distinct kinetics of RNAPII in response to GFs and GCs. MCF10A cells were treated and ChIP-Seq of RNAPII was performed as in Figure 1. Shown are metagene graphs presenting fold change of RNAPII binding following stimulation for 20 or 60 min with EGF, DEX and a combined stimulation (EGF + DEX) for different groups of genes. The different groups were defined as in Figure 8.

Table S1: A list of all module A genes (cooperative module). Note that according to the GO annotation, no gene of the module is involved in cellular motility.

Gene Symbol	Gene Name
CSF3	colony stimulating factor 3 (granulocyte)
CEBPB	CCAAT/enhancer binding protein (C/EBP), beta
NT5DC3	5'-nucleotidase domain containing 3
RAPH1	Ras association (RalGDS/AF-6) and pleckstrin homology domains 1
ZFP36L2	zinc finger protein 36, C3H type-like 2
DUSP1	dual specificity phosphatase 1
PKP2	plakophilin 2
TGM2	transglutaminase 2 (C polypeptide, protein-glutamine-gamma-glutamyltransferase)
RHOB	ras homolog gene family, member B
DCUN1D3	DCN1, defective in cullin neddylation 1, domain containing 3 (<i>S. cerevisiae</i>)
CCNA1	cyclin A1
ERRFI1	ERBB receptor feedback inhibitor 1
ANGPTL4	angiopoietin-like 4
PLAGL2	pleiomorphic adenoma gene-like 2; similar to pleiomorphic adenoma gene-like 2

Table S2: A list of module B genes (the antagonistic module). Genes that are known to be involved in the migration/locomotion, or epithelial to mesenchymal transition (EMT), according to the Gene Ontology database are highlighted (in blue).

Gene Symbol	Gene Name
AMIGO2	adhesion molecule with Ig-like domain 2
ARSJ	arylsulfatase family, member J
BCL3	B-cell CLL/lymphoma 3
BHLHE40	basic helix-loop-helix family, member e40
CMTM7	CKLF-like MARVEL transmembrane domain containing 7
CREB5	cAMP responsive element binding protein 5
CYP27B1	cytochrome P450, family 27, subfamily B, polypeptide 1
DUSP4	dual specificity phosphatase 4

EIF1AD	eukaryotic translation initiation factor 1A domain containing
ENC1	ectodermal-neural cortex (with BTB-like domain)
EOMES	eomesodermin homolog (<i>Xenopus laevis</i>)
EPHA2	EPH receptor A2
EREG	Epiregulin
FLI1	Friend leukemia virus integration 1
GDF15	growth differentiation factor 15
GFPT2	glutamine-fructose-6-phosphate transaminase 2
GJB2	gap junction protein, beta 2, 26kDa
HBEGF	heparin-binding EGF-like growth factor
HES1	hairy and enhancer of split 1, (<i>Drosophila</i>)
ID1	inhibitor of DNA binding 1, dominant negative helix-loop-helix protein
IER3	immediate early response 3
IL1B	interleukin 1, beta
INHBA	inhibin, beta A
KLF10	Kruppel-like factor 10
LONRF3	LON peptidase N-terminal domain and ring finger 3
LRAT	lecithin retinol acyltransferase (phosphatidylcholine--retinol O-acyltransferase)
LRRC8C	leucine rich repeat containing 8 family, member C
MAP3K9	mitogen-activated protein kinase kinase kinase 9
NR4A1	nuclear receptor subfamily 4, group A, member 1
NRG1	neuregulin 1
PHLDA1	pleckstrin homology-like domain, family A, member 1
PHLDA2	pleckstrin homology-like domain, family A, member 2
PLAUR	plasminogen activator, urokinase receptor
PLK3	polo-like kinase 3 (<i>Drosophila</i>)
PTGS2	prostaglandin-endoperoxide synthase 2 (prostaglandin G/H synthase and cyclooxygenase)
PTH1H	parathyroid hormone-like hormone
SERPINB2	serpin peptidase inhibitor, clade B (ovalbumin), member 2
SERTAD4	SERTA domain containing 4
SLC20A1	solute carrier family 20 (phosphate transporter), member 1

STAMBPL1	STAM binding protein-like 1
STK17A	serine/threonine kinase 17a
TRIB1	tribbles homolog 1 (Drosophila)
TRIB3	tribbles homolog 3 (Drosophila)
VEGFA	vascular endothelial growth factor A
XDH	xanthine dehydrogenase

Table S3: Transcription factors whose knockdown affects EGF-dependent migration of mammary cells. Shown are migration-regulating TFs, whose response elements are enriched (p-value < 0.05) at the promoter regions of module B genes. Pscan (<http://159.149.160.51/pscan/>; Jaspasr 2016 database) was used to find over-represented TF binding sites.

TF Symbol	AMD	SD	p-value
NFKB1	0.58	0.10	0.019
TFAP2A	1.22	0.019	0.007
ARNT	0.64	0.29	0.02
REL	1.27	0.03	0.02
MYC	0.74	0.04	0.019
TBP	0.34	0.036	0.0003
JUNB	0.35	0.14	0.002
STAT3	0.63	0.028	0.009